Pergamon

Int. J. Solids Structures Vol. 34, No. 23, pp. 2945–2956, 1997

0020-7683/97 $17.00 + .00

PII: S0020-7683(96)00217-X

NONLINEAR VIBRATIONS OF TIMOSHENKO PIPES CONVEYING FLUID

YIH-HWANG LIN and YAU-KUN TSAI
Department of Mechanical and Marine Engineering, National Taiwan Ocean University, 2 Pei Ning Rd, Keelung, Taiwan 20224, Republic of China

(*Received* 13 *May* 1996; *in revised form* 5 *October* 1996)

Abstract—This paper presents a finite element approach for nonlinear vibration analysis of Timoshenko pipes conveying fluid. An approach using the concept of fictitious loads to account for the kinematic corrections was applied to establish the finite element model, without the need to establish the nonlinear equations of motion. Computation of system responses was carried out by iteratively updating the nodal coordinates until convergence was reached. The formulation and implementation of the approach were verified first by comparing the analysis results with those available in the literature for the case of both slender and short beams undergoing static large deformations and the case of flow induced vibration of a slender cantilever pipe with supercritical flow speeds. Limit cycle and its associated vibration amplitude for the flow induced vibration problem were discussed. Further analysis was conducted for assessment of the effects of flow speed and fluid/pipe mass ratio on the limit cycle vibration amplitude. The influence of slenderness ratio on the limit cycle amplitude was also reported. © 1997 Elsevier Science Ltd.

INTRODUCTION

The dynamic behavior of pipes conveying fluid has received considerable attention in the past. Many articles have been reported in the literature for linear analysis of the flow induced vibration problems (Housner, 1950; Long, 1955; Paidoussis, 1966 and 1975; Paidoussis and Laithier, 1976; Paidoussis *et al.*, 1986; Chu and Lin, 1995). Linear models were used in the past to evaluate the relationship between the critical flow speed and system parameters. The analysis results from the linear models are in serious error when the flow speed is above the critical one and the structure undergoes large deformations (Holmes, 1978). Therefore, nonlinear analysis of pipes conveying fluid due to supercritical flow speed becomes a very important issue to be addressed.

Rousselet and Herrmann (1981) examined dynamic behavior of slender cantilever pipes conveying fluid near critical velocities. For supercritical flow speeds, some of the nonlinear terms discarded in their analysis should be re-examined due to very large amplitudes of motion. Edelstein *et al.* (1986) applied a Galerkin finite element scheme for cantilever pipes conveying fluid with flow velocities larger than the critical value. The classical Bernoulli-Euler beam theory is considered. The scheme requires the correct use of a penalty parameter, which is problem dependent, to ensure numerical stability. Kohnke (1978) presented a procedure for static large deformation analysis of slender frame structures by using the concept of fictitious loads. The static deformation of the structures can be computed by iteratively updating the finite element nodal coordinates, without the need to formulate the nonlinear strain-displacement relationships. In this paper, the concept of fictitious loads is extended for dynamic analysis of cantilever pipes conveying fluid with supercritical flow velocities. The Timoshenko beam theory, which accounts for the effects of shearing deformations and rotary inertia, is considered so that more accurate analysis results than those computed using the classical Bernoulli-Euler beam theory can be obtained in the case of short pipes. In the present approach, no selection of penalty parameter is required. To the authors' knowledge, the present analysis is the first numerical endeavor for nonlinear vibration analysis of Timoshenko pipes conveying fluid by using the simple linear element, without the need to tackle the nonlinear strain-displacement relationships.

The fictitious load approach for nonlinear dynamic analysis requires iterative evaluation of the linear model. The model development of Timoshenko pipes conveying fluid is

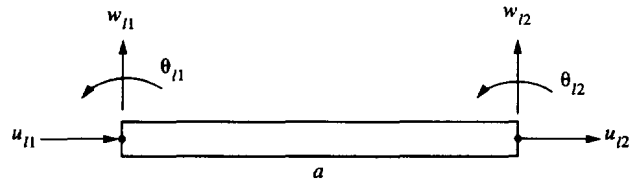

Fig. 1. A two-node Timoshenko frame element with three degrees of freedom per node.

given in the following section, and the procedure for nonlinear dynamic analysis is addressed subsequently. Numerical examples are given to validate the formulation and implementation of the present approach and the effects of fluid mass to pipe mass ratio, slenderness ratio, and fluid flow speed are examined.

MODEL DEVELOPMENT

For static analysis of beams considering the effect of shear deformation, a straight forward energy minimization approach was reported by Narayanaswami and Adelman (1974), which yields correct finite element characteristics without using additional finite element nodal degrees of freedoms. A traditional cubic polynomial can still be used to describe the transverse displacement. The approach is briefly described below for completeness, with additional consideration of the longitudinal effect for large deformation analysis in this work. Extension of the approach for dynamic analysis, taking into account the effect of rotary inertia, is presented subsequently.

Constant shear strain within a cross-section is assumed and is described as:

$$\gamma = \frac{\partial w}{\partial x} - \theta \tag{1}$$

where w denotes transverse displacement of the beam, θ the cross section rotation, and γ the shear strain.

A Timoshenko frame element with two nodes and three degrees of freedom per node is shown in Fig. 1. The displacement fields within an element are interpolated as

$$w = \lfloor N \rfloor \{d_l\}_e, \quad \theta = \lfloor \bar{N} \rfloor \{d_l\}_e, \quad u = \lfloor U \rfloor \{d_l\}_e, \tag{2a}$$

where

$$\lfloor N \rfloor = \lfloor 0\, N_1\, N_2\, 0\, N_3\, N_4 \rfloor, \quad \lfloor \bar{N} \rfloor = \lfloor 0\, \bar{N}_1\, \bar{N}_2\, 0\, \bar{N}_3\, \bar{N}_4 \rfloor,$$
$$\lfloor U \rfloor = \lfloor U_1\, 0\, 0\, U_2\, 0\, 0 \rfloor, \quad \{d_l\}_e = \{u_{l1}\, w_{l1}\, \theta_{l1}\, u_{l2}\, w_{l2}\, \theta_{l2}\}^T, \tag{2b}$$

in which

$$N_1 = 1 - \frac{1}{a(a^2+12g)}(12gx + 3ax^2 - 2x^3),$$

$$N_2 = \frac{1}{a(a^2+12g)}[(a^2+6g)ax - (2a^2+6g)x^2 + ax^3],$$

$$N_3 = \frac{1}{a(a^2+12g)}(12gx + 3ax^2 - 2x^3),$$

$$N_4 = \frac{1}{a(a^2+12g)}[-6gax + (6g-a^2)x^2 + ax^3], \tag{2c}$$

$$\bar{N}_1 = \frac{1}{a(a^2+12g)}(6x^2 - 6ax),$$

$$\bar{N}_2 = \frac{1}{a(a^2+12g)}[a^3+12ga-(4a^2+12g)x+3ax^2],$$

$$\bar{N}_3 = \frac{1}{a(a^2+12g)}(6ax-6x^2),$$

$$\bar{N}_4 = \frac{1}{a(a^2+12g)}[3ax^2-(2a^2-12g)x], \tag{2d}$$

and

$$U_1 = \frac{a-x}{a},$$

$$U_2 = \frac{x}{a}, \tag{2e}$$

where

$$g \equiv \frac{EI}{kGA}, \tag{2f}$$

and $\lfloor N \rfloor$, $\lfloor \bar{N} \rfloor$, and $\lfloor U \rfloor$ denote 1×6 row vectors representing shape functions for transverse displacement, cross-section rotation, and longitudinal displacement, respectively; $\{d_i\}_e$ is the element nodal degrees of freedom vector; a is the beam element length; EI is the bending rigidity; k is the shear coefficient; G is the shear modulus; A is the cross-section area of the beam element; and x is the coordinate along the longitudinal direction of the beam element.

The strain energy including the shear effect for a beam element of length, a, can be described as:

$$V_e = \frac{1}{2}\int_0^a EI\left(\frac{\partial\theta}{\partial x}\right)^2 \mathrm{d}x + \frac{1}{2}\int_0^a EA\left(\frac{\partial u}{\partial x}\right)^2 \mathrm{d}x + \frac{1}{2}\int_0^a kGA\gamma^2 \,\mathrm{d}x. \tag{3}$$

The pipe element stiffness matrix can be obtained directly from the description of strain energy by substitution of eqns (1) and (2) into eqn (3)

$$[k_p]_e = [k_b]_e + [k_a]_e + [k_s]_e, \tag{4a}$$

where

$$[k_b]_e = \int_0^a EI\lfloor \bar{N}_x \rfloor^T \lfloor \bar{N}_x \rfloor \,\mathrm{d}x \tag{4b}$$

represents the effect due to bending strain,

$$[k_a]_e = \int_0^a EA\lfloor U_x \rfloor^T \lfloor U_x \rfloor \,\mathrm{d}x \tag{4c}$$

describes the effect due to axial strain, and

$$[k_s]_e = \int_0^a kGA(\lfloor N_x \rfloor^T - \lfloor \bar{N} \rfloor^T)(\lfloor N_x \rfloor - \lfloor \bar{N} \rfloor)\,dx \tag{4d}$$

accounts for the effect due to shear strain. The subscript x denotes partial differentiation.

For dynamic analysis of a short, sturdy pipe considering both the effects of shearing deformations and rotary inertia, the mass matrix including these effects needs to be determined in addition to the previous development. Using the shape functions described previously, the kinetic energy of the beam can be written as:

$$T_e = \frac{1}{2}\int_0^a m_p\left(\frac{\partial w}{\partial t}\right)^2 dx + \frac{1}{2}\int_0^a m_p\left(\frac{\partial u}{\partial t}\right)^2 dx + \frac{1}{2}\int_0^a \rho_p I\left(\frac{\partial \theta}{\partial t}\right)^2 dx, \tag{5}$$

where m_p, ρ_p, and I are the mass per unit length, mass per unit-volume, and area moment of inertia of the pipe, respectively. Substituting the shape functions and knowing that they are functions of x only, the pipe element mass matrix can be obtained:

$$[m_p]_e = [m_t]_e + [m_a]_e + [m_r]_e, \tag{6a}$$

where $[m_t]_e$ and $[m_a]_e$ represent the traditional mass matrices for transverse and axial inertia effects, whereas $[m_r]_e$ describes the additional rotary inertia effect. These three matrices combined to form the element mass matrix, which can be written as

$$[m_t]_e = \int_0^a \lfloor N \rfloor^T m_p \lfloor N \rfloor\,dx,$$

$$[m_a]_e = \int_0^a \lfloor U \rfloor^T m_p \lfloor U \rfloor\,dx,$$

and

$$[m_r]_e = \int_0^a \lfloor \bar{N} \rfloor^T \rho_p I \lfloor \bar{N} \rfloor\,dx. \tag{6b}$$

Structural damping within the pipe is considered small and hence is neglected. The effects of moving fluid are treated as external forces on the support pipe. The forces turn out to be dependent on the system nodal variables and comprise the centrifugal, Coriolis, and translational inertia forces for a pipe conveying fluid with a constant flowing speed. The element mass, damping, and stiffness matrices for the fluid moving at a constant speed v can be obtained by considering the virtual work done by the fluid forces (Chu and Lin, 1995), with additional consideration of the axial inertia for large deformation analysis of the fluid conveying pipe.

$$[m_f]_e = m_f\int_0^a \lfloor N \rfloor^T \lfloor N \rfloor\,dx + m_f\int_0^a \lfloor U \rfloor^T \lfloor U \rfloor\,dx + \rho_f I_f \int_0^a \lfloor \bar{N} \rfloor^T \lfloor \bar{N} \rfloor\,dx,$$

$$[c_f]_e = m_f v\int_0^a (\lfloor N \rfloor^T \lfloor N_x \rfloor - \lfloor N_x \rfloor^T \lfloor N \rfloor)\,dx,$$

$$[k_f]_e = -m_f v^2 \int_0^a \lfloor N_x \rfloor^T \lfloor N_x \rfloor\,dx, \tag{7}$$

where m_f, ρ_f, and I_f denote the mass per unit length, mass per unit volume, and area moment of inertia of the fluid, respectively. Note that eqn (7) represents a more concise form for

fluid element matrices than that shown in the work by Chu and Lin (1995) by performing additional integration by parts for the original expressions.

PROCEDURE FOR NONLINEAR DYNAMIC ANALYSIS

Eulerian approach is used in this analysis, which does not require the evaluation of nonlinear strain-displacement relationships. The nodal coordinates are updated during the course of computation. Kinematic corrections due to the large deformation of the pipe are accounted for using the fictitious loads. Equations (4), (6), and (7) can be combined to form the dynamic equations of motion in the local coordinate:

$$[m_l]_e\{\ddot{d}_l\}_e + [c_l]_e\{\dot{d}_l\}_e + [k_l]_e\{d_l\}_e = \{r_l\}_e + \{f_l\}_e, \tag{8a}$$

where $\{r_l\}_e$ and $\{f_l\}_e$ denote the external loads, if any, and the fictitious loads on the beam element, respectively, and

$$\begin{aligned} [m_l]_e &= [m_p]_e + [m_f]_e, \\ [c_l]_e &= [c_f]_e, \\ [k_l]_e &= [k_p]_e + [k_f]_e. \end{aligned} \tag{8b}$$

The expressions in the local coordinates can be transformed to the global ones and combined to form the final equations of motion for the entire structure:

$$[M]\{\ddot{D}\} + [C]\{\dot{D}\} + [K]\{D\} = \{R\} + \{F\}, \tag{9a}$$

where

$$\begin{aligned} [M] &= \sum_{j=1}^{n} [T]_j^T [m_l]_e [T]_j, \quad [C] = \sum_{j=1}^{n} [T]_j^T [c_l]_e [T]_j, \\ [K] &= \sum_{j=1}^{n} [T]_j^T [k_l]_e [T]_j, \quad [R] = \sum_{j=1}^{n} [T]_j^T \{r_l\}_j, \\ [F] &= \sum_{j=1}^{n} [T]_j^T \{f_l\}_j, \end{aligned} \tag{9b}$$

in which n is the number of elements used and the coordinate transformation matrix is given as:

$$[T]_j = \begin{bmatrix} \cos\theta_j & \sin\theta_j & 0 & 0 & 0 & 0 \\ -\sin\theta_j & \cos\theta_j & 0 & 0 & 0 & 0 \\ 0 & 0 & 1 & 0 & 0 & 0 \\ 0 & 0 & 0 & \cos\theta_j & \sin\theta_j & 0 \\ 0 & 0 & 0 & -\sin\theta_j & \cos\theta_j & 0 \\ 0 & 0 & 0 & 0 & 0 & 1 \end{bmatrix}. \tag{9c}$$

The procedure for computing the fictitious loads for Bernoulli-Euler beams as reported by Kohnke (1978) is extended here with the additional consideration of shear effect. The fictitious loads can be shown to be:

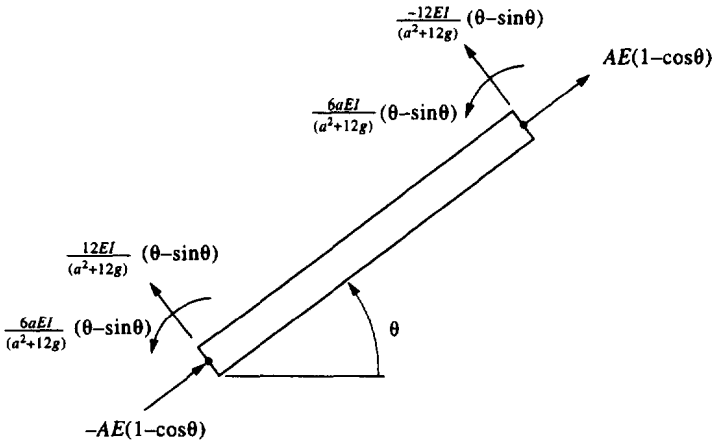

Fig. 2. Local fictitious loads on a Timoshenko frame element.

$$\{f_l\}_e = [k_p]_e\{u_l\} = \begin{Bmatrix} -AE(1-\cos\theta) \\ \dfrac{12EI}{(a^2+12g)}(\theta-\sin\theta) \\ \dfrac{6aEI}{(a^2+12g)}(\theta-\sin\theta) \\ AE(1-\cos\theta) \\ \dfrac{-12EI}{(a^2+12g)}(\theta-\sin\theta) \\ \dfrac{6aEI}{(a^2+12g)}(\theta-\sin\theta) \end{Bmatrix}, \tag{10a}$$

where

$$\{u_l\} = \{0 \;\; 0 \;\; \theta-\sin\theta \;\; a(1-\cos\theta) \;\; 0 \;\; \theta-\sin\theta\}^T. \tag{10b}$$

Figure 2 illustrates the local fictitious loads on an element with an arbitrary orientation. Relative Euclidean norm error in displacements is used to check for convergence, which is defined as

$$e = \frac{\|\{D\}^i\| - \|\{D\}^{i-1}\|}{\|\{D\}^{i-1}\|}, \tag{11}$$

where the superscripts i and $i-1$ denote the present and the previous computed displacements, respectively. Convergence is considered achieved if the error is less than a small quantity ε. In this work, ε is chosen to be 10^{-6}. Figure 3 illustrates the general procedure for nonlinear vibration analysis of pipes conveying fluid.

NUMERICAL RESULTS

Before commencing the study for dynamic analysis, a static analysis test was conducted to validate the formulation and implementation developed in this work. In Fig. 4 are shown the tip displacements of a cantilever beam with rectangular cross-section subjected to a tip load. The geometric nonlinearity due to large deformation was considered. Linear solutions were included for the purpose of comparison. For slender beams, where the Bernoulli-Euler theory is applicable, exact solution is available using the elliptic integral. For short beams, the general purpose finite element package, ANSYS (1995), was used to compute the results

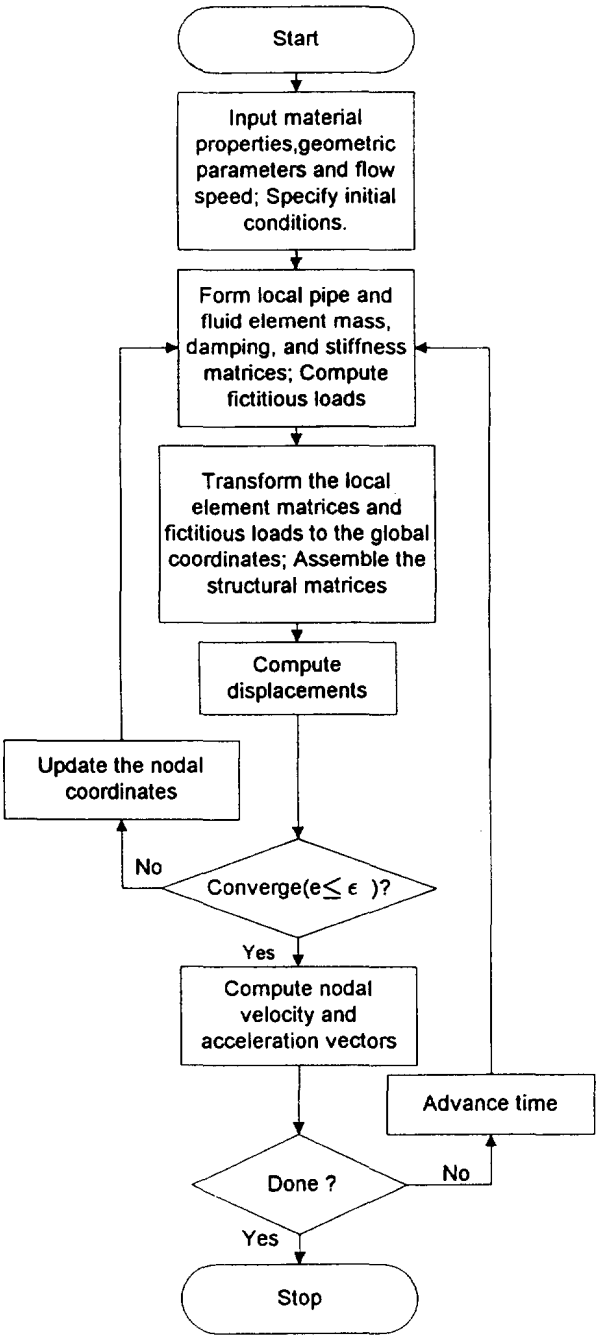

Fig. 3. Flow chart for nonlinear dynamic analysis of pipes conveying fluid.

for comparison. The length to height ratio was taken to be 3 for the short beam case. A total of eight elements was used with the element type BEAM23 being selected. As can be seen in Fig. 4, the analysis results from the present work are in excellent agreement with those computed from exact analysis for slender beams and from ANSYS for short beams.

In this study, the flutter behavior of a cantilever pipe conveying fluid was examined. The numerical data, as used in the earlier work by Edelstein *et al.* (1986), for analysis of a slender cantilever pipe are: $9.525(10^{-3})$ m O.D., $1.5875(10^{-3})$ m wall thickness and 0.6858 m length. Young's modulus is $2.5217(10^{8})$ Pa and the tube and fluid mass densities are 852.59 kg/m^3 and 1000 kg/m^3, respectively. When the fluid flow speed exceeds the critical one, vibration of the pipe grows until a periodic limit cycle is reached. The vibration amplitude and frequency of the limit cycle are determined by giving the pipe an initial disturbance and allowing the pipe vibration to reach a steady state, as illustrated in Fig. 5, where the

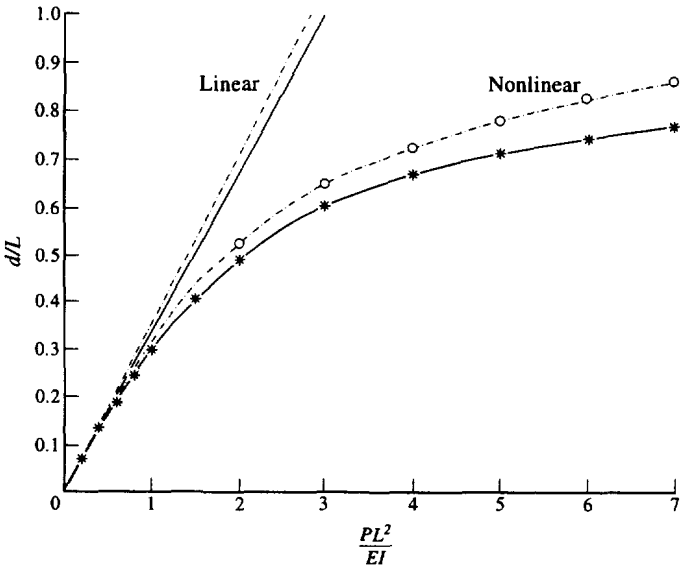

Fig. 4. Tip deflections of a cantilever beam subjected to a tip load. ——, present analysis (Bernoulli-Euler beam); –·–, present analysis (Timoshenko beam), $L/h = 3$; *, elliptic integral solution; ○, ANSYS.

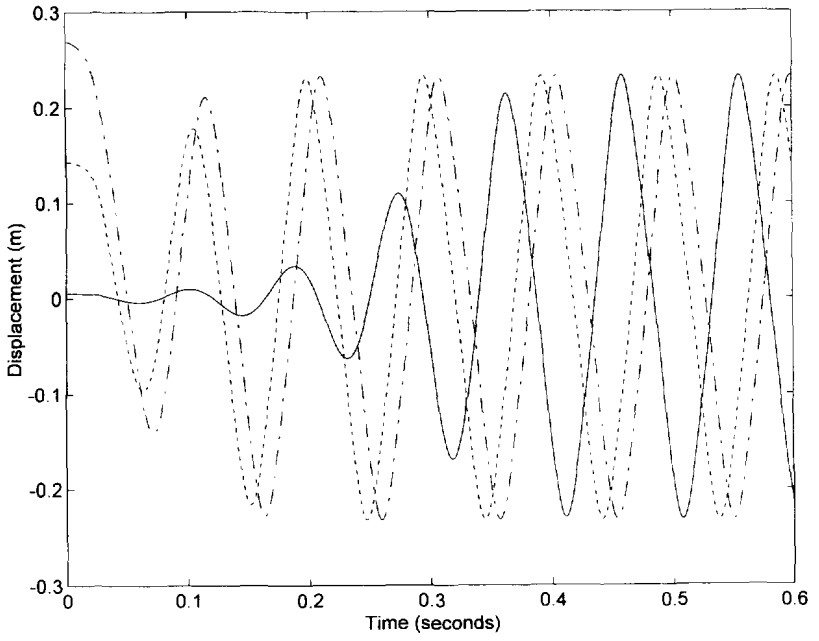

Fig. 5. Tip response of the cantilever pipe at a flow velocity 24.4 m/s with various initial tip displacements. ——, 0.005 m; – – –, 0.14325 m; –·–, 0.26855 m.

tip vibration of the pipe is given with various levels of initial disturbance. The associate phase plane plot is shown in Fig. 6. As can be seen, after only a few cycles of oscillations the pipe reaches the limit cycle due to the supercritical flow velocity. It takes less time for the system response to reach the steady state limit cycle with a larger initial disturbance. If the initial disturbance amplitude is larger than the limit cycle amplitude, the system response is still attracted to the same amplitude of limit cycle, that is the amplitude of limit cycle remains the same disregarding the initial disturbance amplitude as long as it is within the elastic range.

In Figs 7 and 8 are shown the present analysis results in comparison with those obtained by experiments (Chen and Jendrzejczyk, 1985) and by the Galerkin scheme (Edelstein *et al.*, 1986). The pipe is difficult to excite at subcritical flow velocities. Large oscillations occur as the flow velocity is increased to the intrinsic flutter flow velocity. Large

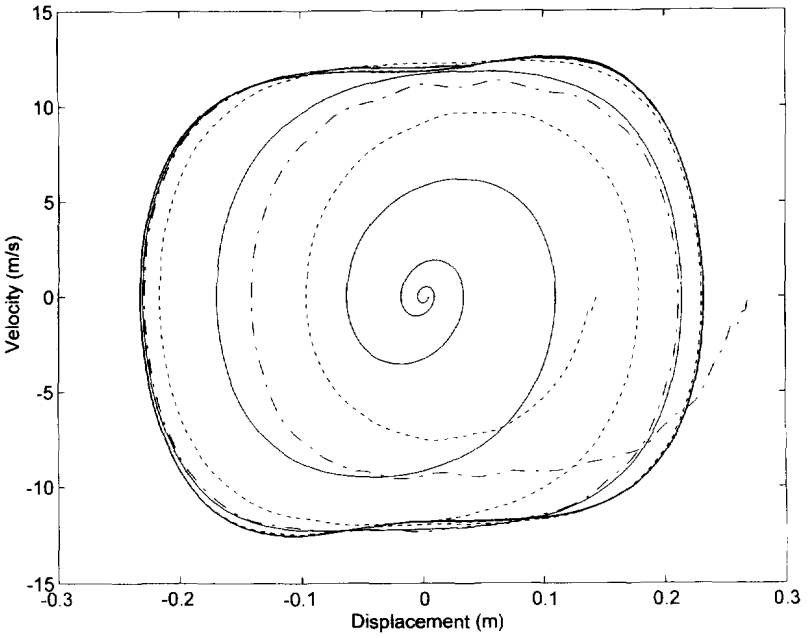

Fig. 6. Phase plane plot for the system analyzed in Fig. 5. ——, 0.005 m; – – –, 0.14325 m; –·–, 0.26855 m.

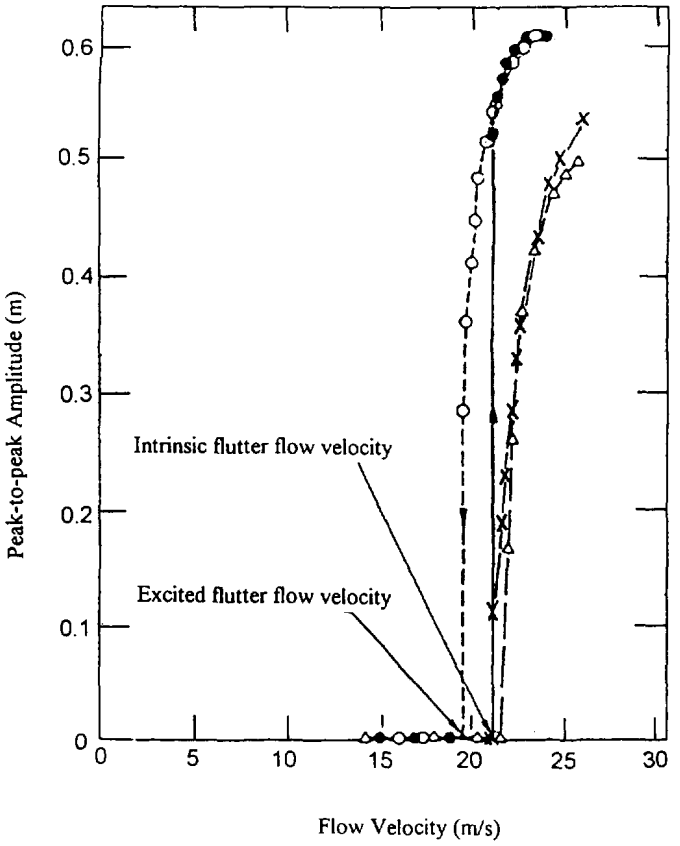

Fig. 7. Effect of flow velocity on limit cycle peak-peak vibration amplitude. X, present analysis; △, (Edelstein *et al.*, 1986); ●, increasing flow; ○, decreasing flow (Chen and Jendrzejczyk, 1985).

oscillations of the pipe do not stop at the intrinsic flutter flow velocity as the flow velocity is decreased, but at a smaller flow velocity called excited flutter flow velocity (Chen and Jendrzejczyk, 1985). The numerical results and the experimental data agree well qualitatively. The discrepancy may be attributed to some non-ideal conditions in experiment,

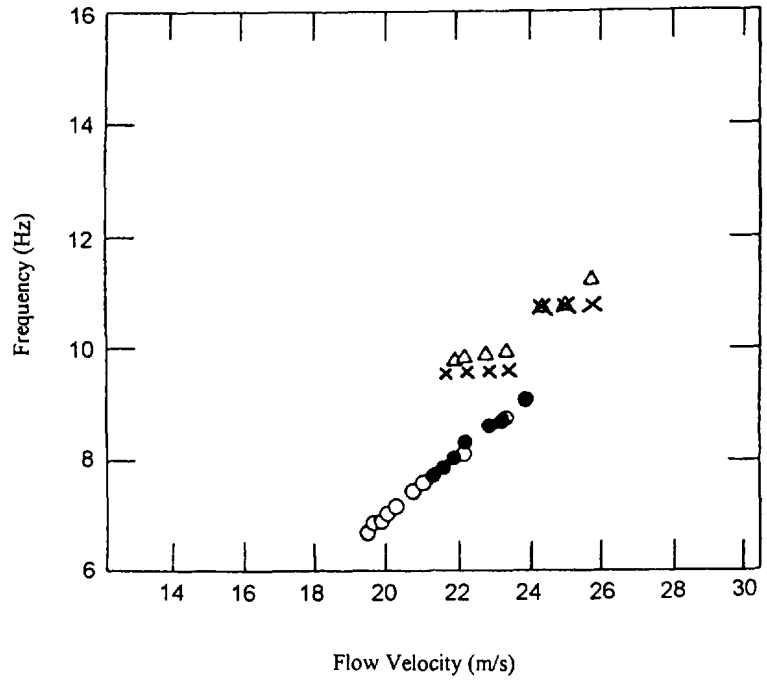

Fig. 8. Effect of flow velocity on limit cycle frequency of oscillation. Key as in Fig. 7.

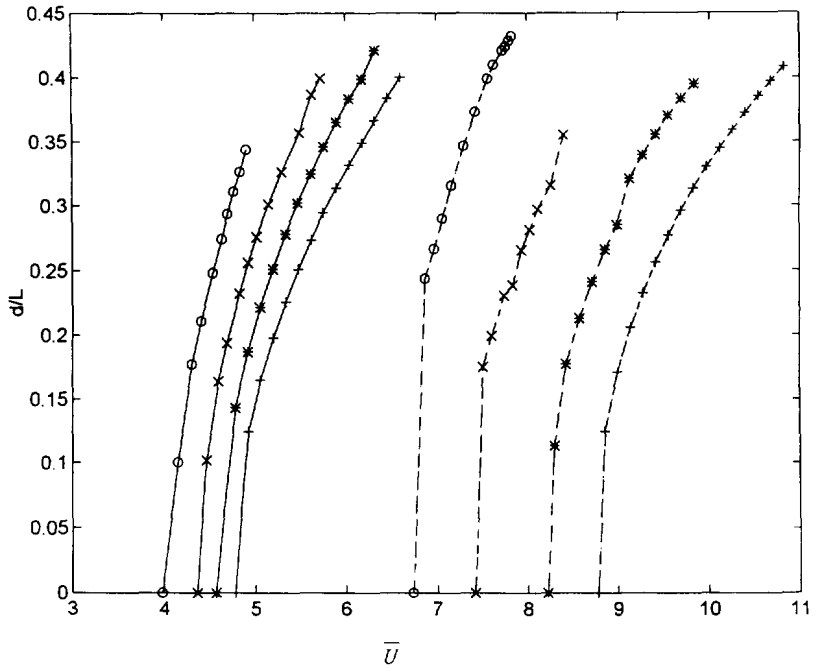

Fig. 9. Normalized amplitude of oscillation versus the normalized flow velocity of a cantilever pipe with various slenderness and mass ratios. ——, $\beta = 0.1$; – – –, $\beta = 0.4$; ○, $\Lambda = 100$; X, $\Lambda = 200$; *, $\Lambda = 500$; +, Bernoulli-Euler theory.

such as non-rigid inlet end, internal fluid pressure, and flow field variations, etc. The overall feature can be found to be in good agreement.

In Fig. 9 are shown the further assessments of the effects of flow speed and mass ratio of fluid to the support pipe on limit cycle vibration amplitude, while taking into account the influences of shear deformations and rotary inertia. The analysis results using the classical Bernoulli-Euler beam theory are also included for reference. The dimensionless quantities are defined as:

$$\beta = \frac{m_f}{m_f + m_p}, \quad \bar{U} = vL\sqrt{\frac{m_f}{EI}}, \quad \Lambda = \frac{kGAL^2}{EI}, \tag{12}$$

where L is the pipe length; β is the mass ratio; $\bar{U}$ is the normalized flow speed; and Λ is the slenderness ratio. As shown in Fig. 7, vibration amplitude for subcritical flow speed is very small, and hence only the limit cycle amplitudes for supercritical speeds are given here. As can be seen in Fig. 9, for a fixed flow speed, the vibration amplitude estimated using the Bernoulli-Euler theory is smaller than that predicted using the more advanced Timoshenko beam theory with various slenderness ratios. This is to be expected in that the former classical theory assumes infinite shear rigidity and neglects the effect of rotary inertia, and hence the system is stiffer than the actual one. Note that vibration amplitude increases drastically once the flow speed exceeds the critical one. This is especially so for a system with a higher mass ratio and a smaller slenderness ratio. The importance of using the Timoshenko beam theory, as opposed to the classical Bernoulli-Euler theory, for predicting the limit cycle behavior is more appreciated as the slenderness ratio becomes smaller.

CONCLUSIONS

A procedure has been presented to solve nonlinear vibration problems of Timoshenko pipes conveying fluid. The approach is rather convenient to apply in that only linear elements are required and the geometric nonlinearity due to large deformations can be treated by including appropriate fictitious loads for kinematic corrections and by successively updating the nodal coordinates. No explicit nonlinear strain-displacement relationships need to be established, and the formulation of nonlinear structural matrices to describe the equations of motion is no longer necessary. Numerical simulation results from the proposed approach are in excellent agreement with those obtained from exact solution for static large deformation analysis of a slender beam. As for short beam study, excellent agreement has also been observed when compared with the ANSYS analysis. Comparison of the analysis results from this work with those obtained from a previously reported experiment and from a Galerkin approach reveals that the present procedure is sound. The procedure presented in this paper is capable of analyzing fluid-conveying pipes with supercritical flow speeds, taking into account the effects of shearing deformations and rotary inertia.

Challenges still remain for dynamic analysis of pipes conveying fluid, despite the fact that a considerable amount of articles has been generated in this field. For supercritical flow speeds, the flow pattern may be quite complex and the fluid/structure interactions pose an interesting and complicated problem to solve. Such effect is not included in the present analysis and further dedicated research is called for to address such complex issue. Improved accuracy may be obtained by considering the flow speed being coupled to the pipe motion rather than a prescribed known parameter. By doing so, the governing equations of motion for both the support pipe and the moving fluid become coupled due to large deformations. A more advanced flow field representation may also be considered by applying the potential flow theory, where the fluid dynamic forces are connected to the normal pressure on the support pipe. The ultimate endeavor on the flow field is the determination of the turbulent flow profile, whose connection to the large deformations of the support pipe is still not well understood. As the slenderness ratio becomes smaller, two concerns arise. For thin-walled pipes, thin shell theory and three-dimensional flow theory are required to accurately model the system. For thick-walled pipes, the system may require the full equations of elasticity theory for accurate modeling. Moreover, active/passive vibration control of fluid-conveying pipes exhibiting excessive vibration is also a fascinating and important subject to explore. Reports on the subject are scarce to date.

Acknowledgement—The authors are grateful to the National Science Council (NSC), Taiwan, ROC, for the financial support under the contract NSC 85-2212-E-019-002.

REFERENCES

ANSYS User's Manual for Revision 5.1 (1995) Swanson Analysis Systems, Inc., Houston, Pennsylvania.

Chen, S. S. and Jendrzejczyk, J. A. (1985) General characteristics, transition, and control of instability of tubes conveying fluid. *Journal of Acoustical Society of America* **77,** 887–895.

Chu, C. L. and Lin, Y. H. (1995) Finite element analysis of fluid-conveying Timoshenko pipes. *Shock and Vibration* **2,** 247–255.

Edelstein, W. S., Chen, S. S. and Jendrzejczyk, J. A. (1986) A finite element computation of the flow-induced oscillations in a cantilevered tube. *Journal of Sound and Vibration* **107,** 121–129.

Holmes, P. J. (1978) Pipes supported at both ends cannot flutter. *Journal of Applied Mechanics* **45,** 619–622.

Housner, G. W. (1950) Bending vibration of a pipe line containing flowing fluid. *Journal of Applied Mechanics* **72,** 229–232.

Kohnke, P. C. (1978) Large deflection analysis of frame structures by fictitious forces. *International Journal of Numerical Methods in Engineering* **12,** 1279–1294.

Long, R. H., Jr. (1955) Experimental and theoretical study of transverse vibration of a tube containing flowing fluid. *Journal of Applied Mechanics* **77,** 65–68.

Narayanaswami, R. and Adelman, H. M. (1974) Inclusion of transverse shear deformation in finite element displacement formulation. *AIAA Journal* **12**(11), 1613–1614.

Paidoussis, M. P. (1966) Dynamics of flexible slender cylinders in axial flow. *Journal of Fluid Mechanics* **26,** 717–736.

Paidoussis, M. P. (1975) Flutter of conservative systems of pipes conveying incompressible fluid. *Journal of Mechanical Engineering Science* **17,** 19–25.

Paidoussis, M. P. and Laithier, B. E. (1976) Dynamics of Timoshenko beams conveying fluid. *Journal of Mechanical Engineering Science* **18,** 210–220.

Paidoussis, M. P., Luu, T. P. and Laithier, B. E. (1986) Dynamics of finite-length tubular beams conveying fluid. *Journal of Sound Vibration* **106,** 311–331.

Rousselet, J. and Herrmann, G. (1981) Dynamic behaviour of continuous cantilevered pipes conveying fluid near critical velocities. *Journal of Applied Mechanics* **48,** 943–947.